Catalytic growth of silica nanoparticles in controlled shapes at planar liquid/liquid interfaces

Nurxat Nuraje,[a] Kai Su[b] and Hiroshi Matsui*[a]

Received (in Gainesville, FL, USA) 9th August 2007, Accepted 14th September 2007
First published as an Advance Article on the web 2nd October 2007
DOI: 10.1039/b712260h

The shape of silica nanoparticles is controlled when they are synthesized at liquid/liquid interfaces; the combination of organic and aqueous phases that form the interface can change the shape of silica into a triangle, cube, or rod.

In recent years, material scientists have extensively investigated novel ways to control the shape of nanoparticles.[1] Controlling shapes of nanoparticles is becoming extremely important in various practical applications since chemical and physical properties of nanoparticles can be tunable by their shapes.[2,3] For example, different shapes of nanoparticles have different absorption properties so that the shape control can create a new set of colors of the nanoparticles in addition to the size, useful for medical imaging. For another application of shape-controlled nanoparticles in catalysis: when Pt nanoparticles were grown in a tetrahexahedral shape, their catalytic activity was enhanced because these nanoparticles had many high-index facets that served as active sites for breaking chemical bonds.[4] Here, we report a novel method to control the shape of nanoparticles by reacting precursors at planar liquid/liquid interfaces. By simply changing the combination of organic and aqueous solvents that formed the interface, this interfacial growth technique yielded different shapes of silica nanoparticles as triangles, cubes, rods, or ropes.

In general, non-spherical nanoparticles can be grown by modulating the relative surface energies between faces of nuclei.[2,5] While various dry and wet methods have produced nanoparticles in well-defined shapes, wet chemical methods have an advantage of controlling the shape by influencing growth rates on specific faces of nuclei at the nucleation stage *via* capping of these faces with surfactants, ions, or biomolecules.[6–15] In all cases, the shape control becomes more effective when the nucleation and the growth rates slow down so that these surfactants have enough time to absorb particular faces; by this face-selective capping, the growth rate for each face is no longer equal, which could yield non-spherical nanoparticles.

Interfaces between two immiscible liquids, such as the surfaces of droplets, have been shown to be ideal platforms for the assembly of colloidal nanoparticles[16–19] but there were fewer reports on growing inorganic nanoparticles at planar immiscible interfaces.[20] However, experimental studies of chemical reactions at liquid/liquid interfaces at the microscopic level are still in their infancy and particle growth at the liquid/liquid interface has not been explored to control shape.[21,22] In fact, the planar liquid/liquid interface has significant potential for controlled particle growth since this soft interface lacks fixed nucleation sites which gives capping ions freedom to target certain faces of nuclei and the interfacial tension retards particle growth rates to control their morphologies.[23] The slowing of nuclear kinetics at the interface is caused by the lower stability of small nuclei due to the change in interfacial tension between two different phases.[24] While the slower nucleation kinetics have been observed at planar liquid/liquid interfaces, there are few reports taking advantage of this to control the shape of nanoparticles at the interfaces. Here, our strategy for the shape control of nanoparticles is to apply various positive and negative ions at planar liquid/liquid interfaces where the nucleation kinetics are slow enough for these ions to absorb and change the growth rate on particular faces, and these face-selective ion absorptions tethered the shape of resulting nanoparticles *via* hydrolysis and condensation (Fig. 1). While silica and other nanoparticles were assembled into various shapes by the surfactant supramolecular assembly method in a bulk single-phase solution,[25,26] here we report an alternative method for nanoparticle shape control: the liquid/liquid interfacial nanoparticle growth method. In this report, we selected silica as a model growth system

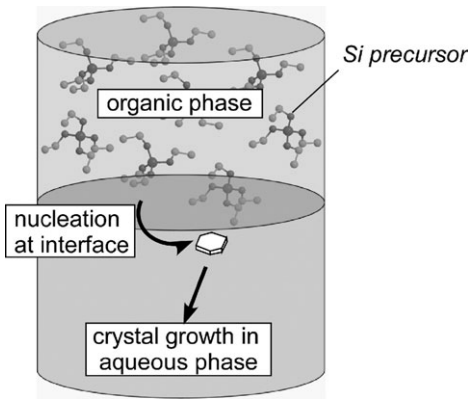

Fig. 1 Illustration of the scheme to grow silica in various shapes at planar liquid/liquid interfaces. The aqueous phase contains ions that not only catalyze the condensation but also cap a specific face of the nuclei to slow particle growth at the interface.

[a] *Department of Chemistry, City University of New York, Hunter College and The Graduate Center, 695 Park Ave, New York, NY 10065, USA. E-mail: hmatsui@hunter.cuny.edu; Fax: +1 (212) 772 5332; Tel: +1 (212) 650 3918*
[b] *Department of Chemistry, City University of New York, College of Staten Island, 2800 Victory Blvd., Staten Island, NY 10314, USA. E-mail: sukai2002us@yahoo.com; Fax: +1 (718) 982 3910; Tel: +1 (718) 982 2000*

since its growth mechanisms in acid and base catalyses are well characterized. While previously the interfacial synthesis strategy has been applied to grow polymers in controlled morphologies,[21,27] the application of interfacial growth to inorganic nanoparticle syntheses in controlled shapes has not been explored extensively.

In this planar liquid/liquid interfacial growth of silica, the Si precursor, tetraethyl orthosilicate (TEOS), and catalyst were loaded in different layers; TEOS in an organic layer and the catalyst in an aqueous layer. As the alkoxide precursor from the organic phase contacted and reacted with the catalyst at the liquid/liquid interface, silica particles were formed by hydrolysis and condensation. The intermediate species condensed from silanol $[Si(OH)_n]_m$ clusters were hydrophilic and therefore the growth of silica nanoparticles was driven in the direction from the organic layer to the aqueous layer. The interfacial experiments were conducted under five different conditions with TEOS as the precursor. In the interfacial syntheses with acid catalysis, HCl or HNO_3 solution was employed as the aqueous phase and *n*-butanol as the organic phase. In the interfacial syntheses with base catalysis, we applied NaOH or NH_4OH as the aqueous phase and *n*-butanol as the organic phase. Chloroform was also applied as the organic phase to further slow down the growth rate of silica at the liquid/liquid interface.

With the acid catalysis, hydrolysis of the TEOS precursor without an interface by stirring the solution yielded branched silica wires as shown in Fig. 2a. This branched wire growth without any particular shape control was also observed in sol–gel growth methods in homogeneous solutions containing acid catalysis.[26] However, the shape of the silica particles was changed as the precursor was hydrolyzed at the liquid/liquid interface between the organic phase and the aqueous phase. When the TEOS precursor was in the *n*-butanol (top layer) and the acid catalyst HCl was in the aqueous phase (bottom layer), silica nanorods of 40 nm in width and several micrometres in length were readily formed toward the aqueous layer (Fig. 2b). While these nanowires formed at the liquid/liquid interface were not branched out as observed in the homogeneous sol–gel system, the formation of the similar elongated structure between them indicates that there is only a weak influence on the shape control of the silica nanoparticles with the HCl/butanol interfacial system. This is due to fast silica condensation with the acid catalyst and under these conditions ions at the interface have little time to influence the shape of the silica nanoparticles by absorbing on specific faces of the silica nuclei.

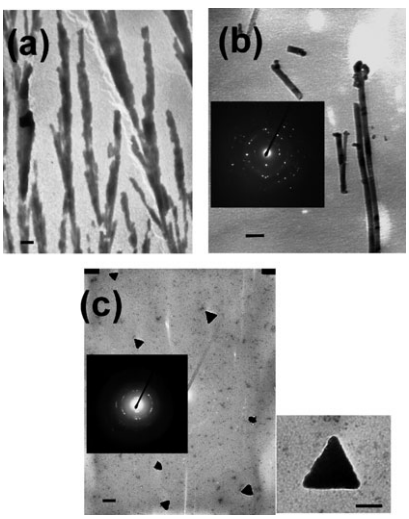

Fig. 2 TEM images of (a) silica grown with no interface by stirring the aqueous solution of HCl, (b) silica grown at the HCl/butanol interface, (c) silica grown at the HCl/$CHCl_3$ interface (right: magnified TEM image, scale bar = 100 nm). Scale bar = 200 nm. Insets show the electron diffraction patterns.

However, a striking difference was observed when the organic solvent containing the TEOS precursor was changed from *n*-butanol to chloroform for the interfacial silica growth with acid catalysis. In this case, the TEOS precursor in the chloroform phase in the bottom layer was hydrolyzed at the interface by the acid catalyst HCl that originated from the aqueous phase in the top layer, which is the reversed configuration of the HCl/butanol interface. This HCl/$CHCl_3$ interface produced triangle-shaped silica nanoparticles as shown in Fig. 2c. The triangular nanoparticle was 200 ± 20 nm on each side. It should be noted that there were areas on the TEM grids where the spherical form of silica was more dominant. The electron diffraction pattern (inset of Fig. 2c) showed the polycrystalline nature of the nanoparticles and these silica nanoparticles could contain the α-quartz domain based on this diffraction pattern. Although the condensation was still the rate-determining step in the acid catalysis interface, the aprotic organic solvent, $CHCl_3$, made a significant impact on the nucleation kinetics on specific nucleus faces otherwise silica nanoparticles would not grow in a particularly defined shape. The major difference in applying $CHCl_3$ as the organic layer is the silica growth rate at the interface. In order for the silica growth to occur, silanols from the organic layer of chloroform need to cross the interface toward the aqueous layer and undergo the condensation; however $CHCl_3$ could retard the transfer from the organic to the aqueous layers since this aprotic solvent hydrogen bonds to electrophilic deprotonated silanols at the acidic interface.[28] Due to this reduced rate for the overall condensation reaction, chlorine ions at the interface have enough time to selectively adsorb onto certain faces of the silica nanoparticles at the nucleation, which controls the shape of the resulting particles. Previously, the adsorption of chlorine ions onto the ⟨111⟩ face produced triangular Cu nanoparticles,[29] and the triangular silica nanoparticles grown at the interface between the $CHCl_3$ organic layer and the HCl aqueous layer could undergo the same shape-control mechanism. It should be noted that the control experiment in Fig. 2a, which failed to grow the shaped particles in a bulk solution without the interface, suggests that the interface plays an important role on the particle shape; if those particles are simply grown by means of the salt condensation during the drying process, we should observe the trianglular particles when the bulk solution of precursor and catalyst was dried.

When the TEOS precursor was hydrolyzed in homogeneous media with base catalysis without the interface by stirring the solution, large polydispersed silica particles were grown as shown in Fig. 3a. This type of amorphous particle growth

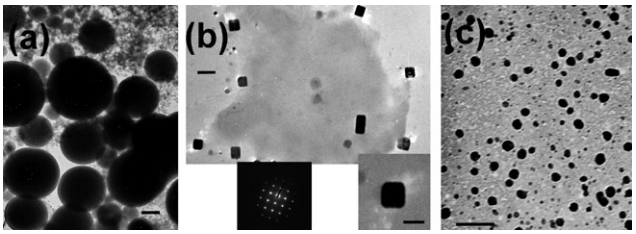

Fig. 3 TEM images of (a) silica grown with no interface by stirring the aqueous solution of NaOH, scale bar = 200 nm, (b) silica grown at the NaOH/butanol interface, scale bar = 70 nm (right inset: magnified TEM image, scale bar = 50 nm; left inset: the electron diffraction pattern), (c) silica grown at the NH_4OH/butanol interface, scale bar = 200 nm.

without any particular shape control was also observed previously in homogeneous sol–gel growth methods with base catalysis.[28] However, when silica was grown at the liquid/liquid interface with the base catalyst, NaOH, in the aqueous layer and the TEOS precursor in the organic layer of *n*-butanol, the shape of the nanoparticles was cubic and the average size of the cubic nanoparticles was 100 ± 10 nm each side (Fig. 3b). Some of nanoparticles in Fig. 3b were in a rectangular form since two cubic nanoparticles aggregated side by side. The diffraction pattern in Fig. 3b indicates that this silica nanoparticle is more crystalline as compared to the triangular particles produced at the $HCl/CHCl_3$ interface, and the pattern has a close match with α-crystabolite. When NH_4OH was applied as the base catalyst in the aqueous layer, the polydispersed spherical nanoparticles appeared and their structure was amorphous. Since polydispersed spherical nanoparticles grown at the NH_4OH/butanol interface resemble the nanoparticles grown without the interface, the NH_4OH catalyst at the liquid/liquid interface has no influence on the shape of the silica. In the case of the base catalysis growth, *n*-butanol and chloroform yielded the same particle shapes at the interface. Among the interfaces with the base catalysts, only the NaOH/butanol interfacial system tethered the particle shape to cubic because the stronger base NaOH produced higher ion concentrations at the interface, which can cap certain faces of the silica nuclei more effectively to control the shape of resulting silica nanoparticles. Previously, the shape of titania nanoparticles has been controlled by capping them with Me_4N^+. This small cation could stabilize the negative charges of titania at the nucleation stage *via* electrostatic interactions and yielded titania nanoparticles with defined shapes.[30] Sodium oleate and sodium stearate could also control the shape of titania nanoparticles to cubic by capping ⟨100⟩ and ⟨001⟩ faces.[31] For this interfacial growth of silica with base catalysis, abundant sodium ions at the NaOH/butanol interface could influence the silica growth on these faces under the characteristic slow condensation at the liquid/liquid interface. Since the influence of the NH_4OH/butanol interface on the particle shape of silica is much weaker than the NaOH/butanol interface, the cationic concentration is also important, in addition to the slowing growth kinetics, to control the shape of the nanoparticles at the liquid/liquid interface. It should be noted that the same phenomenon was observed as the lower anionic concentration at the weak acid/$CHCl_3$ interface failed to influence the shape of the silica nanoparticles.

In summary, negative and positive ions at the liquid/liquid interface could change the growth rates on specific faces of silica nanoparticles under the slow nucleation conditions and this interfacial growth technique yielded different shapes of silica nanoparticles as triangles, cubes, rods, or ropes by simply changing the combination of organic and aqueous solvents that formed the interface. The aim of this study is to demonstrate that the particle shape can be changed at the liquid/liquid interface when the shape cannot be controlled under the same conditions in the bulk single-phase solution. The interfacial synthesis has an advantage in slowing the particle growth, which increases the probability of surfactants and ions influencing the resulting shapes. Silica was used as a model in this study, and this interfacial method will become more practical if the same shape control can be achieved for more important materials such as quantum dots. In theory, this interfacial synthesis should be applicable to control the shapes of various inorganic nanoparticles whose precursors can be dissolved in organic solutions and whose catalysts or reducing agents can be dissolved in aqueous solutions. Therefore, this interfacial growth method has potential to tether the shape of inorganic nanoparticles without using complex multiple synthetic processes. It should be noted that this method enables one to not only tether nanoparticle shapes but also provide means to investigate the effect of solvents on fundamental inorganic nanoparticle growth mechanisms under controlled environments. And last, we would like to emphasize that our interfacial method can be served as an alternative method to the existing colloidal synthesis for the shape control of nanoparticles, and there is potential that our interfacial method could be applied to controlling the shape of some systems whose shape is difficult to change by traditional colloidal methods. And the combination of those two methods could enhance the precision of the shape control.

Experimental

The silica precursor, tetraethyl orthosilicate (TEOS, 98%, Sigma-Aldrich) was dissolved in the organic solvent, *n*-butanol (Fisher) or $CHCl_3$ (Sigma-Aldrich), in a 1 M concentration. To form the liquid/liquid interface with the *n*-butanol organic layer, first a 0.1 M aqueous solution of acid or base, HCl, HNO_3 (Fisher), NH_4OH (Sigma-Aldrich), or NaOH (Acros Organics), was added to a vial, and then 5 ml of the TEOS–*n*-butanol solution was added slowly along the wall of the vial without disturbing the interface. In these interfacial systems, the organic phase of *n*-butanol was located as the top layer. To form the liquid/liquid interface with the $CHCl_3$ organic layer, first 5 ml of the TEOS–$CHCl_3$ solution was added to a vial, and then 5 ml of the 0.1 M HCl solution was added slowly along the wall of the vial without disturbing the interface. In these interfacial systems, the organic phase of $CHCl_3$ was located as the bottom layer. After two days, the aqueous layer containing the silica nanoparticles was washed and centrifuged. The silica nanoparticles extracted from the aqueous layer were then dried on carbon coated copper grids at room

temperature for TEM and electron diffraction measurements at an acceleration voltage of 100 kV (JEOL 1200 EX).

Acknowledgements

The authors acknowledge gratefully the support from: the US Department of Energy: DE-FG-02-01ER45935 and the National Science Foundation CARRER Award: ECS-0103430. Hunter College infrastructure is supported by the National Institutes of Health and the RCMI program: G12-RR-03037. Part of this work was completed in the Core Facility for Imaging, Cell and Molecular Biology at Queens College, CUNY.

References

1 V. F. Puntes, K. M. Krishnan and A. P. Alivisatos, *Science*, 2001, **291**, 2115–2117.
2 Y.-W. Jun, J.-S. Choi and J. Cheon, *Angew. Chem., Int. Ed.*, 2006, **45**, 3414–3439.
3 Y. N. Xia, P. D. Yang, Y. G. Sun, Y. Y. Wu, B. Mayers, B. Gates, Y. D. Yin, F. Kim and Y. Q. Yan, *Adv. Mater.*, 2003, **15**, 353–389.
4 N. Tian, Z.-Y. Zhou, S.-G. Sun, Y. Ding and Z. L. Wang, *Science*, 2007, **316**, 732–735.
5 J. W. Mullin, *Crystalization*, Butterworth-Heinmann, Woburn, MA, 1997.
6 A. M. Belcher, X. H. Wu, R. J. Christensen, P. K. Hansma, G. D. Stucky and D. E. Morse, *Nature*, 1996, **381**, 56–58.
7 J. Tang, X. Cui, Y. Liu and X. Yang, *J. Phys. Chem. B*, 2005, **109**, 22244–22249.
8 L. F. Gou and C. J. Murphy, *Nano Lett.*, 2003, **3**, 231–234.
9 R. C. Jin, Y. W. Cao, C. A. Mirkin, K. L. Kelly, G. C. Schatz and J. G. Zheng, *Science*, 2001, **294**, 1901–1903.
10 R. R. Naik, S. J. Stringer, G. Agarwal, S. E. Jones and M. O. Stone, *Nat. Mater.*, 2002, **1**, 169–172.
11 S. Brown, M. Sarikaya and E. Johnson, *J. Mol. Biol.*, 2000, **299**, 725–735.
12 S. Mann, D. D. Archibald, J. M. Didymus, T. Douglas, B. R. Heywood, F. C. Meldrum and N. J. Reeves, *Science*, 1993, **261**, 1286–1292.
13 Y. J. Han, L. M. Wysocki, M. S. Thanawala, T. Siegrist and J. Aizenberg, *Angew. Chem., Int. Ed.*, 2005, **44**, 2386–2390.
14 H. Colfen and M. Antonietti, *Angew. Chem., Int. Ed.*, 2005, **44**, 5576–5591.
15 M. Umetsu, M. Mizuta, K. Tsumoto, S. Ohara, S. Takami, H. Watanabe, I. Kumagai and T. Adschiri, *Adv. Mater.*, 2005, **17**, 2571–2575.
16 J. T. Russell, Y. Lin, A. Boker, L. Su, P. Carl, H. Zettl, J. B. He, K. Sill, R. Tangirala, T. Emrick, K. Littrell, P. Thiyagarajan, D. Cookson, A. Fery, Q. Wang and T. P. Russell, *Angew. Chem., Int. Ed.*, 2005, **44**, 2420–2426.
17 O. D. Velev, K. Furusawa and K. Nagayama, *Langmuir*, 1996, **12**, 2374–2384.
18 B. P. Binks and J. H. Clint, *Langmuir*, 2002, **18**, 1270–1273.
19 A. D. Dinsmore, M. F. Hsu, M. G. Nikolaides, M. Marquez, A. R. Bausch and D. A. Weitz, *Science*, 2002, **298**, 1006–1009.
20 X. Song, S. Sun, W. Zhang, H. Yu and W. Fan, *J. Phys. Chem. B*, 2004, **108**, 5200–5205.
21 K. Su, N. Nuraje, L. Zhang, I. W. Chu, R. Peetz, H. Matsui and N. L. Yang, *Adv. Mater.*, 2007, **19**, 669–672.
22 I. Benjamin, *Chem. Rev.*, 1996, **96**, 1449–1475.
23 T. Nakashima and N. Kimizuka, *J. Am. Chem. Soc.*, 2003, **125**, 6386–6387.
24 C. Johans, P. Liljeroth and K. S. Kontturi, *Phys. Chem. Chem. Phys.*, 2002, **4**, 1067–1071.
25 H. Yang, N. Coombs and G. A. Ozin, *Nature*, 1997, **386**, 692–695.
26 T. Nakanishi, W. Schmitt, T. Michinobu, D. Kurth and K. Ariga, *Chem. Commun.*, 2006, 5982–5984.
27 J. X. Huang and R. B. Kaner, *Angew. Chem., Int. Ed.*, 2004, **43**, 5817–5821.
28 C. J. Brinker and G. Scherer, *Sol-Gel Science*, Academic Press, Boston, MA, 1990.
29 A. Filankembo, S. Giorgio, I. Lisiecki and M. P. Pileni, *J. Phys. Chem. B*, 2003, **107**, 7492–7500.
30 A. Chemseddine, H. Jungblut and S. Boulmaaz, *J. Phys. Chem.*, 1996, **100**, 12546–12551.
31 T. Sugimoto, X. P. Zhou and A. Muramatsu, *J. Colloid Interface Sci.*, 2003, **259**, 53–61.

